Supporting Information

An efficient medium-bandgap nonfullerene acceptor for organic solar cells

Qishi Liu,[‡a,b] Ke Jin,[‡b] Wenting Li,[b] Zuo Xiao,*[,b] Ming Cheng,[c] Yongbo Yuan,[d] Shengwei Shi,[e] Zhiwen Jin,*[,f] Feng Hao,*[,g] Shangfeng Yang*[,a] and Liming Ding*[,b]

[a]*Hefei National Laboratory for Physical Sciences at Microscale, Key Laboratory of Materials for Energy Conversion (CAS), Department of Materials Science and Engineering, University of Science and Technology of China, Hefei 230026, China. E-mail: sfyang@ustc.edu.cn*

[b]*Center for Excellence in Nanoscience (CAS), Key Laboratory of Nanosystem and Hierarchical Fabrication (CAS), National Center for Nanoscience and Technology, Beijing 100190, China. E-mail: xiaoz@nanoctr.cn; ding@nanoctr.cn*

[c]*Institute for Energy Research, Jiangsu University, Zhenjiang 212013, China.*

[d]*School of Physics & Electronics, Central South University, Changsha 410083, China.*

[e]*School of Materials Science and Engineering, Wuhan Institute of Technology, Wuhan 430205, China.*

[f]*School of Physical Science and Technology, Lanzhou University, Lanzhou 730000, China. E-mail: jinzw@lzu.edu.cn*

[g]*School of Materials and Energy, University of Electronic Science and Technology of China, Chengdu 611731, China. E-mail: haofeng@uestc.edu.cn*

1. General characterization

^{1}H and ^{13}C NMR spectra were measured on a Bruker Avance-400 spectrometer. Absorption spectra were recorded on a Shimadzu UV-1800 spectrophotometer. Cyclic voltammetry was done by using a Shanghai Chenhua CHI620D voltammetric analyzer under argon in an anhydrous ODCB/CH_3CN (9:1) solution of tetra-n-butylammonium hexafluorophosphate (0.1 M). IBCT was dissolved in the solution. A glassy-carbon electrode was used as the working electrode, a platinum-wire was used as the counter electrode, and a Ag/Ag^+ electrode was used as the reference electrode. All potentials were corrected against Fc/Fc^+. Single-crystal XRD analysis for BCT was performed on a Rigaku AFC10 diffractometer. AFM was performed on a Multimode microscope (Veeco) using tapping mode.

2. Synthesis

All reagents were purchased from J&K Co., Aladdin Co., Innochem Co., SunaTech Co. and other commercial suppliers. All reactions dealing with air- or moisture-sensitive compounds were carried out by using standard Schlenk techniques. IDT-CHO[1] was prepared according to literature.

1H-Benzo[b]cyclopenta[d]thiophene-1,3(2H)-dione. To a solution of benzo[*b*]thiophene-2-carboxylic acid (178 mg, 1 mmol) in chloroform (6 mL) was added thionyl chloride (0.3 mL, 4 mmol) and 3 drops dry DMF. The reaction was stirred at 65 °C for one hour. After removal of the solvent and excess thionyl chloride, the intermediate, benzo[b]thiophene-2-carbonyl chloride, was obtained and used for next step without purification. To a solution of benzo[b]thiophene-2-carbonyl chloride in dry chloroform (6 mL) was added $AlCl_3$ (798 mg, 6 mmol) under argon. The mixture was stirred at room temperature for 30 min. Then, malonyl dichloride (846 mg, 6 mmol) was added into the mixture. The reaction was stirred at 65 °C overnight. After cooling to room temperature, the mixture was poured into hydrochloric acid (1 M) slowly. The pH of the solution was tuned to 7 by adding $NaHCO_3$. The crude product extracted from dichloromethane was purified via column chromatography (silica gel) by using CH_2Cl_2:petroleum ether (1:1) as eluent to give **1H-benzo[b]cyclopenta[d]thiophene-1,3(2H)-dione** as a faint yellow solid (67 mg, 33%). ^{1}H NMR ($CDCl_3$, 400 MHz, δ/ppm): 8.39-8.43 (m, 1H), 7.96-8.00 (m, 1H), 7.59-7.63 (m, 2H), 3.55 (s, 2H). ^{13}C NMR (DMSO, 100 MHz, δ/ppm): 191.15, 190.90, 157.65, 151.88, 147.11, 129.92, 129.14, 127.31, 125.06, 124.89, 49.16. ESI MS (m/z): 201.1 (M^+).

2-(1-Oxo-1,2-dihydro-3H-benzo[b]cyclopenta[d]thiophen-3-ylidene)malononitrile (BCT). To a mixed solution of 1H-benzo[b]cyclopenta[d]thiophene-1,3(2H)-dione (202 mg, 1 mmol) and malononitrile (99 mg, 1.5 mmol) in DMSO (10 mL) was added sodium acetate (123 mg, 1.5 mmol). The mixture was stirred for one hour at room temperature. Then, hydrochloric acid was added to tune the pH to ~1. The solid was filtered and purified via column chromatography (silica gel) by using CH_2Cl_2 as eluent to give **BCT** as a yellow solid (212 mg, 85%). ^{1}H NMR ($CDCl_3$, 400 MHz, δ/ppm): 8.40 (d, *J* = 7.7 Hz, 1H), 7.99 (d, *J* = 8.0 Hz, 1H), 7.61-7.69 (m, 2H), 3.98 (s, 2H). ^{13}C NMR (DMSO, 100 MHz, δ/ppm): 189.23, 164.45, 157.11, 148.38, 147.70, 129.91, 129.26, 127.74, 125.02, 124.47, 112.13, 76.20, 46.58. ESI MS (m/z): 250.1 (M^+). Single crystals of **BCT** were obtained by slowly diffusing hexane into its THF solution. Formula: $C_{14}H_5N_2OS$; formula weight: 249.26; crystal system: monoclinic; space group: *P* 21/n; color of crystal: yellow; unit cell parameters: a = 7.3820(1) Å, b = 21.4301(4) Å, c = 7.7843(2) Å, α = 90°, β = 114.060(2)°, γ = 90°, V = 1124.46(4) Å^3; temperature for data collection: 169.99(10) K; *Z* = 4; final *R* indices [I >2σ(I)]: *R1* = 0.0335, *wR2* = 0.0928; GOF on F^2: 1.074. The crystallographic data have been deposited in Cambridge Crystallographic Data Centre (**CCDC-1955137**).

IBCT. To a solution of IDT-CHO (100 mg, 0.1mmol) in DMSO (20 mL) was added BCT (125 mg, 0.5 mmol) and pyridine (0.5 mL) at room temperature. The mixture was heated to reflux for 48 h. After removal of the solvent, the crude product was purified via column chromatography (silica gel) by using $CHCl_3$ as eluent to give **IBCT** as a black solid (102 mg, 70%). ^{1}H NMR ($CDCl_3$, 400 MHz, δ/ppm): 8.72 (s, 2H), 8.45-8.46 (m, 2H), 7.97-7.99 (m, 2H), 7.66 (s, 2H), 7.61-7.63 (m, 4H), 7.60 (s, 2H), 2.05-2.10 (m, 4H), 1.92-1.97 (m, 4H), 1.13-1.23 (m, 56H), 0.80-0.93 (m, 20H). ^{13}C NMR ($CDCl_3$, 100 MHz, δ/ppm): 182.90, 158.62, 157.98, 156.94, 156.16, 154.53, 147.48, 143.96, 139.73, 137.61, 136.82, 135.51, 130.43, 129.32, 127.36, 125.08, 123.96, 123.66, 115.67, 114.06, 113.70, 68.89, 54.29, 39.03, 31.88, 29.91, 29.59, 29.54, 29.32, 29.30, 24.39, 22.64, 14.08. MALDI-TOF MS (m/z): 1346.7 (M^+).

3. NMR

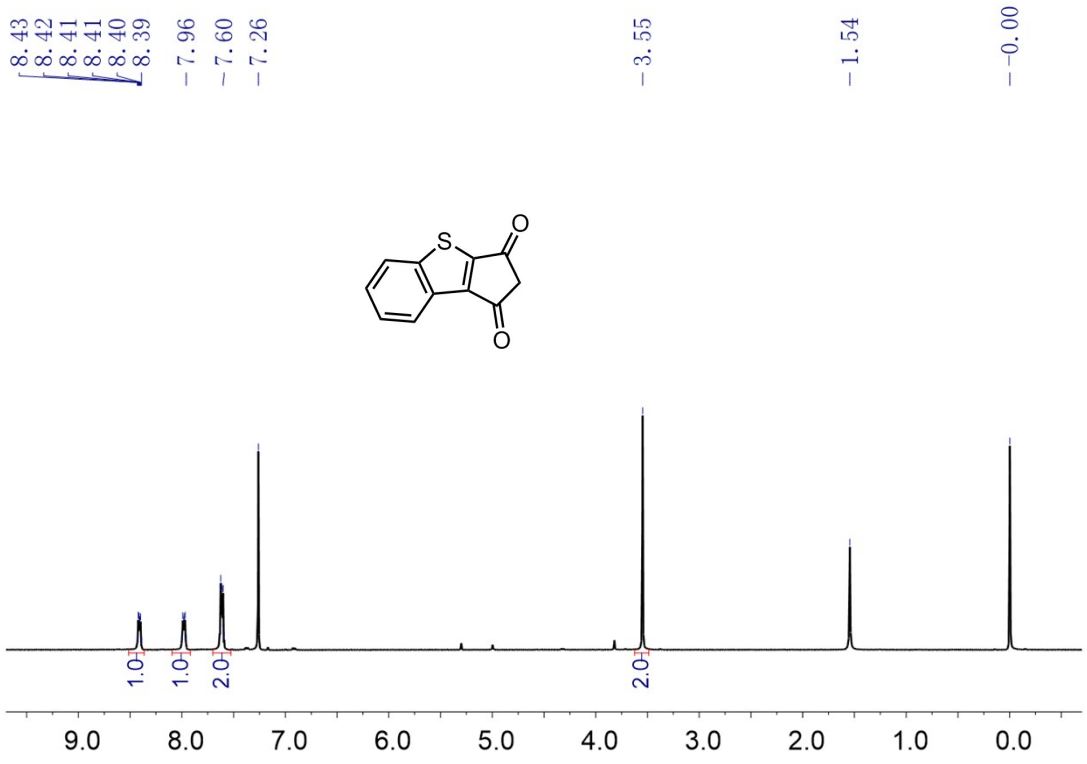

Fig. S1 ^{1}H NMR spectrum of **1H-benzo[b]cyclopenta[d]thiophene-1,3(2H)-dione.**

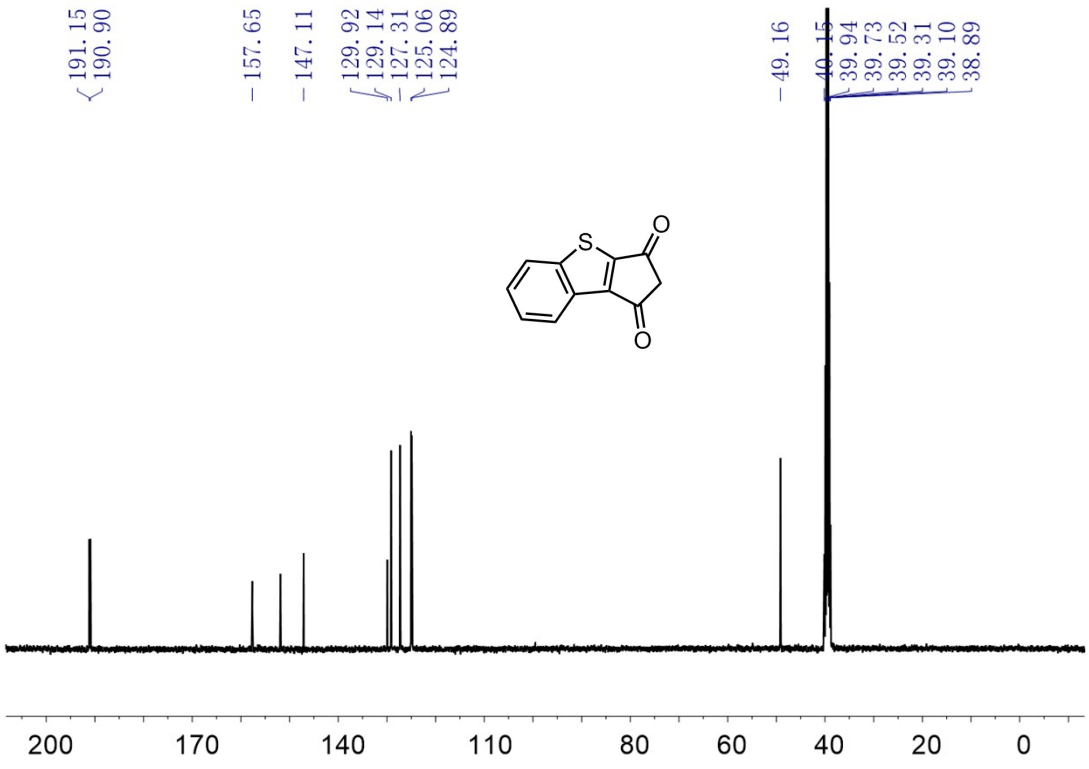

Fig. S2 ^{13}C NMR spectrum of **1H-benzo[b]cyclopenta[d]thiophene-1,3(2H)-dione.**

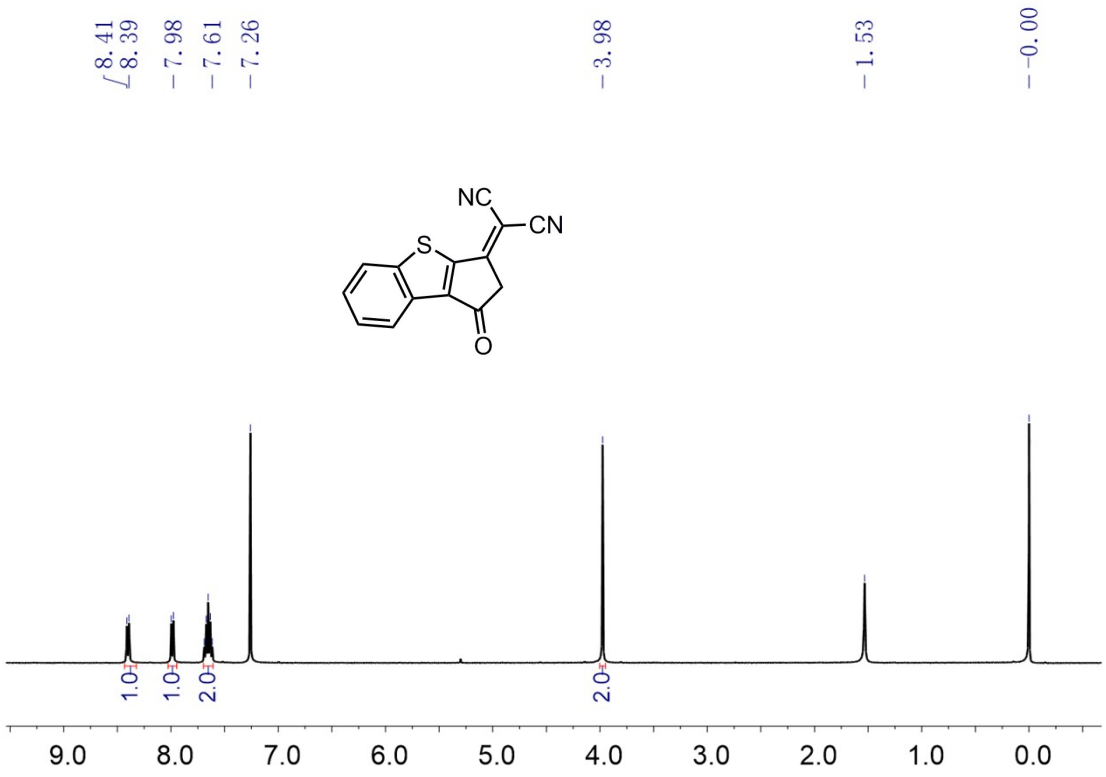

Fig. S3 ^{1}H NMR spectrum of **BCT.**

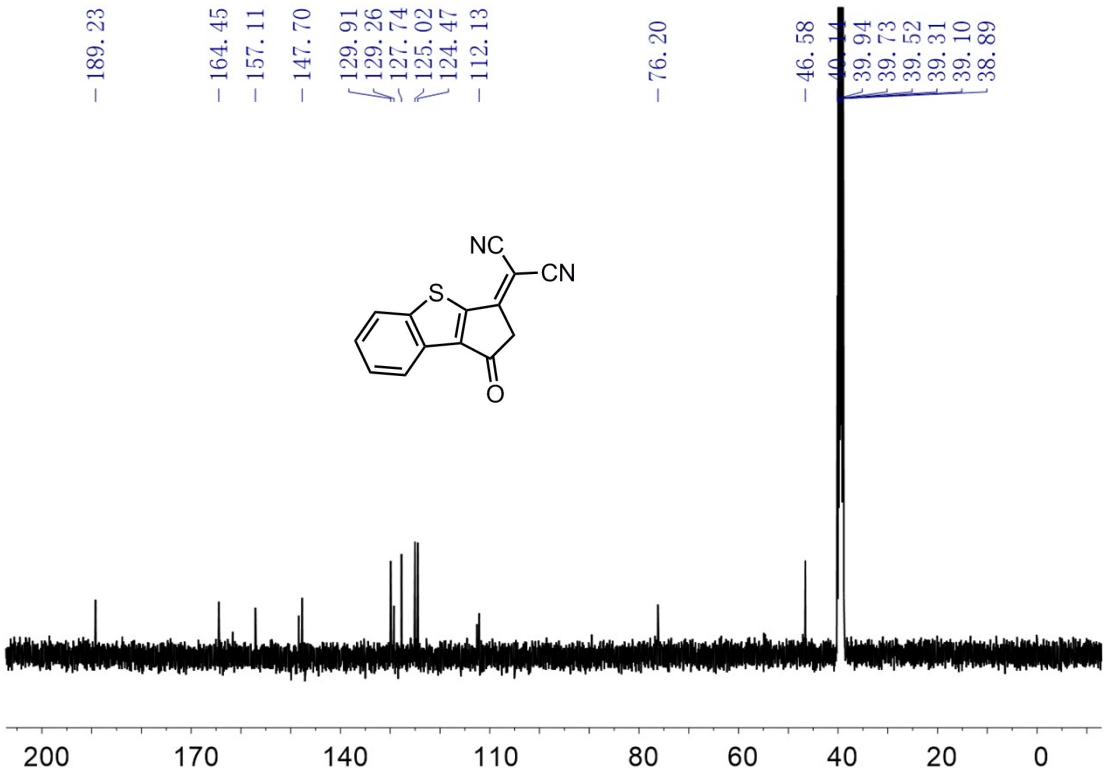

Fig. S4 ^{13}C NMR spectrum of **BCT.**

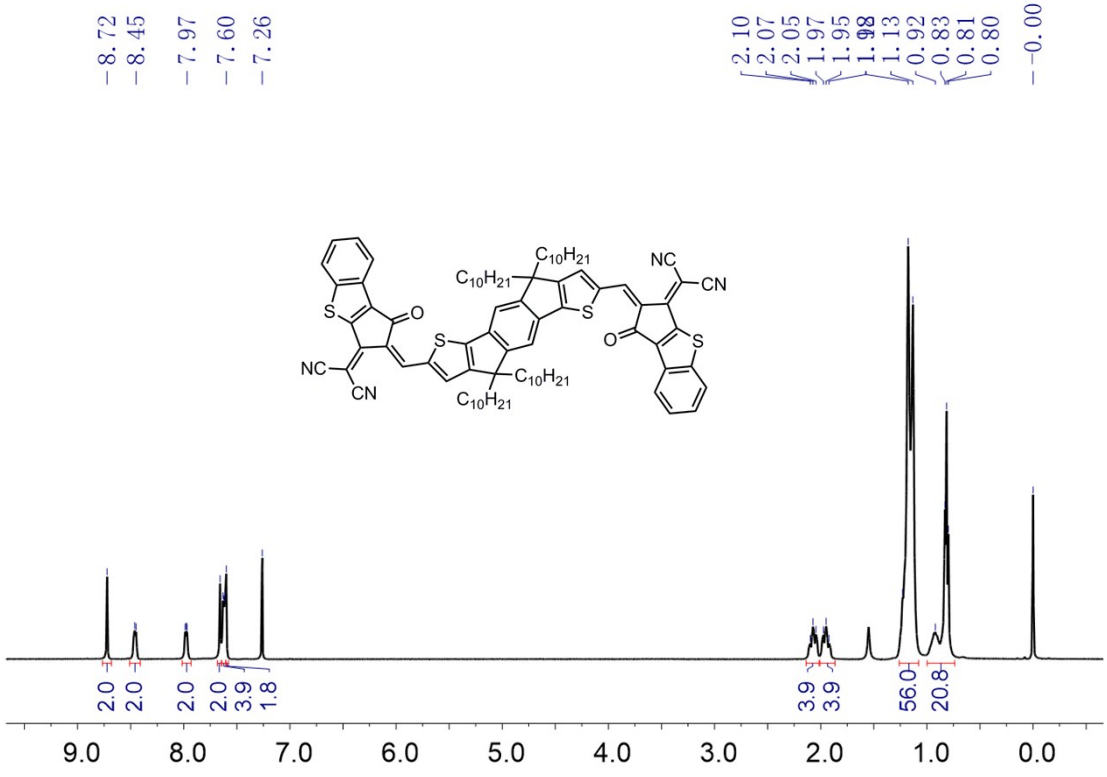

Fig. S5 ^{1}H NMR spectrum of **IBCT.**

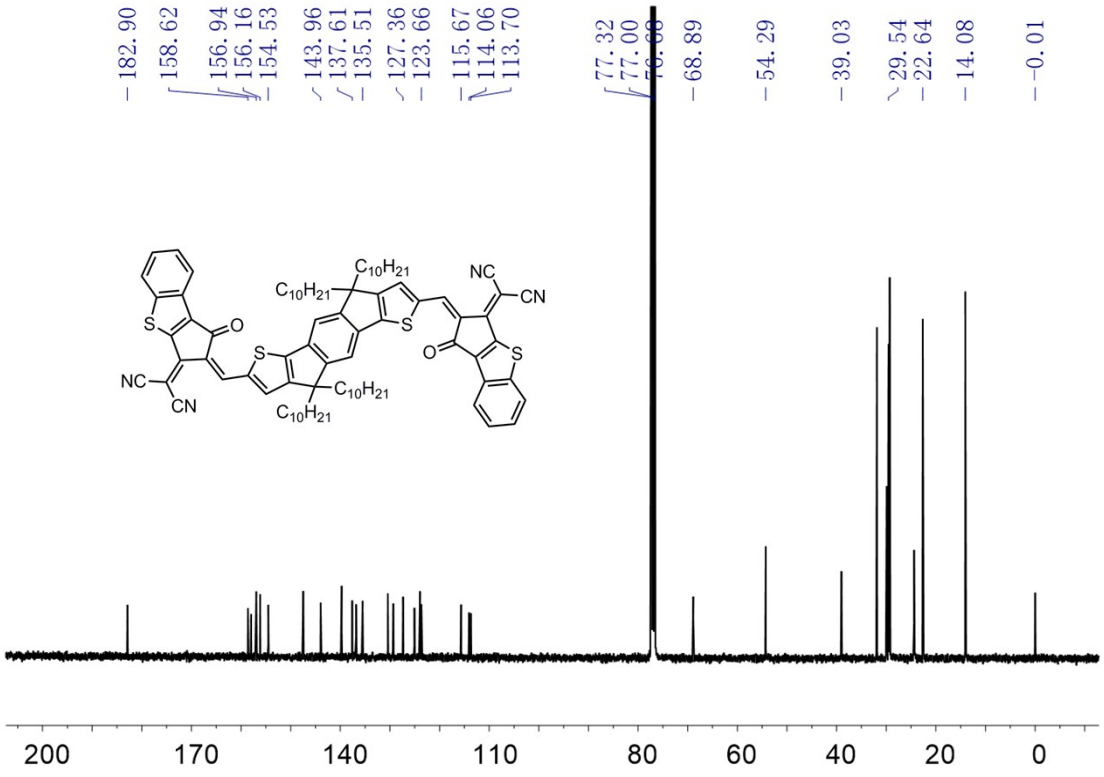

Fig. S6 ^{13}C NMR spectrum of **IBCT.**

4. CV

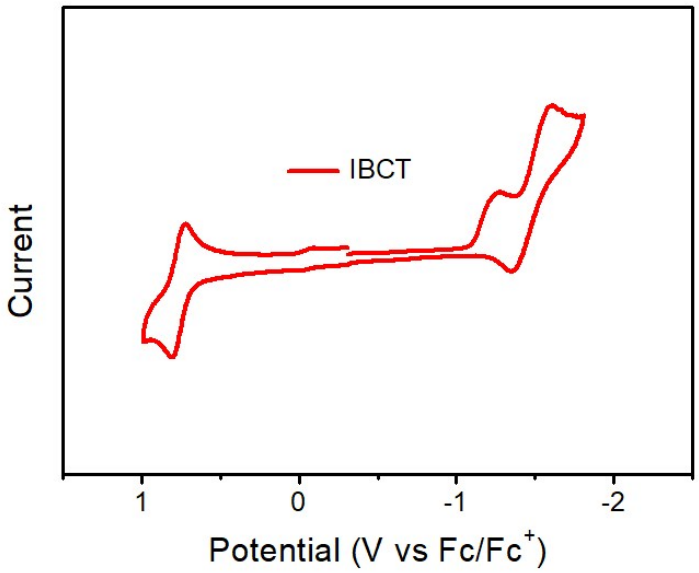

Fig. S7 Cyclic voltammogram for IBCT.

5. Device fabrication and measurements

Conventional solar cells

A 30 nm thick PEDOT:PSS (Clevios™ P AI 4083) layer was made by spin-coating an aqueous dispersion onto ITO glass (4000 rpm for 30 s). PEDOT:PSS substrates were dried at 150 °C for 10 min. A L1:IBCT blend in chloroform (CF) with or without chloronaphthalene (CN) was spin-coated onto PEDOT:PSS. PDIN (2 mg/mL) in MeOH:AcOH (1000:3) was spin-coated onto active layer (5000 rpm for 40 s). Al (~100 nm) was evaporated onto PDIN through a shadow mask (pressure ca. 10^{-4} Pa). The effective area for the devices is 4 mm^2. The thicknesses of the active layers were measured by using a KLA Tencor D-120 profilometer. *J-V* curves were measured by using a computerized Keithley 2400 SourceMeter and a Xenon-lamp-based solar simulator (Enli Tech, AM 1.5G, 100 mW/cm^2). The illumination intensity of solar simulator was determined by using a monocrystalline silicon solar cell (Enli SRC2020, 2cm×2cm) calibrated by NIM. The external quantum efficiency (EQE) spectra were measured by using a QE-R3011 measurement system (Enli Tech).

Hole-only devices

The structure for hole-only devices is ITO/PEDOT:PSS/active layer/MoO_3/Al. A 30 nm thick PEDOT:PSS layer was made by spin-coating an aqueous dispersion onto ITO glass (4000 rpm for 30 s). PEDOT:PSS substrates were dried at 150 °C for 10 min. A L1:IBCT blend in CF with or without CN was spin-coated onto PEDOT:PSS. Finally, MoO_3 (~6 nm) and Al (~100 nm) was successively evaporated onto the active layer through a shadow mask (pressure ca. 10^{-4} Pa). *J-V* curves were measured by using a computerized Keithley 2400 SourceMeter in the dark.

Electron-only devices

The structure for electron-only devices is Al/active layer/Ca/Al. Al (~80 nm) was evaporated onto a glass substrate. A L1:IBCT blend in CF with or without CN was spin-coated onto Al. Ca (~5 nm) and Al (~100 nm) were successively evaporated onto the active layer through a shadow mask (pressure ca. 10^{-4} Pa). *J-V* curves were measured by using a computerized Keithley 2400 SourceMeter in the dark.

Tandem solar cells

A 30 nm thick PEDOT:PSS (Clevios™ P AI 4083) layer was made by spin-coating an aqueous dispersion onto ITO glass (4000 rpm for 30 s). PEDOT:PSS substrates were dried at 150 °C for 10 min. A L1:IBCT blend (16 mg/mL in CF with 0.7 vol% CN) was spin-coated onto PEDOT:PSS (2500 rpm for 30 s). The thickness of the L1:IBCT layer is ~140 nm. ZnO nanoparticles[2] were spin-coated onto L1:IBCT layer. M-n-

PEDOT:PSS (n-PEDOT:PSS (Organcon™ N-1005) diluted 7-folds with 5 vol% n-propyl alcohol) was spin-coated onto ZnO (4000 rpm for 30 s). Then, M-PEDOT:PSS (PEDOT:PSS (Clevios™ P AI 4083) diluted 1-fold with 5 vol% n-propyl alcohol) was spin-coated onto M-n-PEDOT:PSS (4000 rpm for 30 s). A L1:Y6 blend (16 mg/mL in CF) was spin-coated onto M-PEDOT:PSS (4000 rpm for 30 s). The thickness of the L1:Y6 layer is ~110 nm. PDIN (2 mg/mL) in MeOH:AcOH (1000:3) was spin-coated onto active layer (5000 rpm for 40 s). Al (~100 nm) was evaporated onto PDIN through a shadow mask (pressure ca. 10^{-4} Pa). The effective area for the devices is 4 mm^2. *J-V* curves were measured by using a computerized Keithley 2400 SourceMeter and a Xenon-lamp-based solar simulator (Enli Tech, AM 1.5G, 100 mW cm^{-2}). The illumination intensity of solar simulator was determined by using a monocrystalline silicon solar cell (Enli SRC2020, 2cm×2cm) calibrated by NIM. The EQE spectra were measured by using a QE-R3011 measurement system (Enli Tech). It must be noticed that a 550 and 850 nm light bias was selected to excite the front and rear cells to measure the EQE of the rear and front cells, respectively.

6. Optimization of device performance

Table S1 Optimization of D/A ratio for L1:IBCT conventional solar cells.[a]

D/A [w/w]	V_{oc} [V]	J_{sc} [mA/cm^2]	FF [%]	PCE [%]
1:0.8	1.02	13.13	70.4	9.42 (9.08)[b]
1:1	1.02	13.76	71.7	10.05 (9.67)
1:1.2	1.02	15.07	73.5	11.26 (10.95)
1:1.4	1.02	14.37	72.6	10.65 (10.11)

[a]Blend solution: 16 mg/mL in CF with 0.7 vol% CN; spin-coating: 3500 rpm for 30 s.
[b]Data in parentheses are averages for 8 cells.

Table S2 Optimization of active layer thickness for L1:IBCT conventional solar cells.[a]

Thickness [nm]	V_{oc} [V]	J_{sc} [mA/cm^2]	FF [%]	PCE [%]
159	1.01	13.40	68.3	9.25 (8.95) [b]
138	1.02	13.78	71.5	10.08 (9.78)
125	1.02	15.07	73.5	11.26 (10.95)
112	1.02	13.71	72.1	10.11 (9.98)

[a]D/A ratio: 1:1.2 (w/w); blend solution: 16 mg/mL in CF with 0.7 vol% CN.
[b]Data in parentheses are averages for 8 cells.

Table S3 Optimization of CN content for L1:IBCT conventional solar cells.[a]

CN [vol%]	V_{oc} [V]	J_{sc} [mA/cm^2]	FF [%]	PCE [%]
0	1.02	13.43	69.8	9.58 (9.39)[b]
0.5	1.02	13.90	71.2	10.11 (9.71)
0.7	1.02	15.07	73.5	11.26 (10.95)
1.0	1.01	14.17	69.6	9.98 (9.65)

[a]D/A ratio: 1:1.2 (w/w); blend solution: 16 mg/mL in CF; spin-coating: 3500 rpm for 30 s.

[b]Data in parentheses are averages for 8 cells.

7. Exciton dissociation probabilities

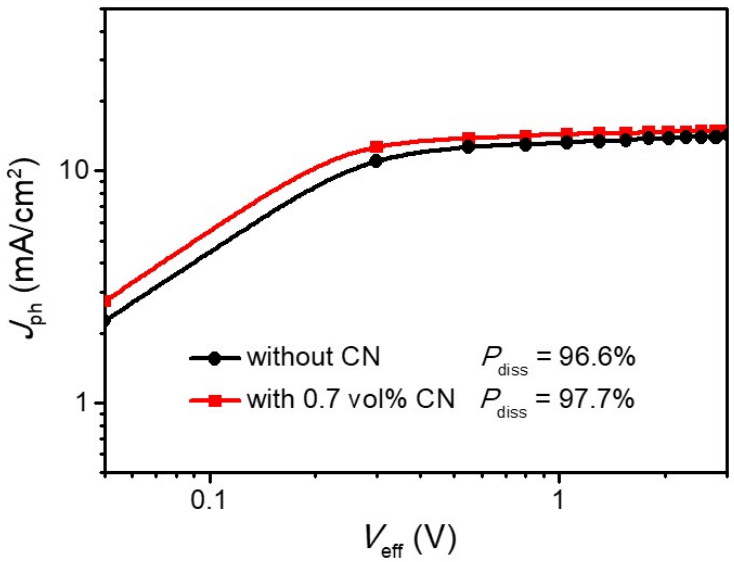

Fig. S8 J_{ph}-V_{eff} plots.

8. SCLC

Charge carrier mobility was measured by SCLC method. The mobility was determined by fitting the dark current to the model of a single carrier SCLC, which is described by:

$$J = \frac{9}{8}\varepsilon_0\varepsilon_r\mu\frac{V^2}{d^3}$$

where J is the current density, μ is the zero-field mobility of holes (μ_h) or electrons (μ_e), ε_0 is the permittivity of the vacuum, ε_r is the relative permittivity of the material, d is the thickness of the blend film, and V is the effective voltage ($V = V_{appl} - V_{bi}$, where V_{appl} is the applied voltage, and V_{bi} is the built-in potential determined by electrode work function difference). Here, $V_{bi} = 0.1$ V for hole-only devices, $V_{bi} = 0$ V for electron-only devices.[3] The mobility was calculated from the slope of $J^{1/2}$-V plots.

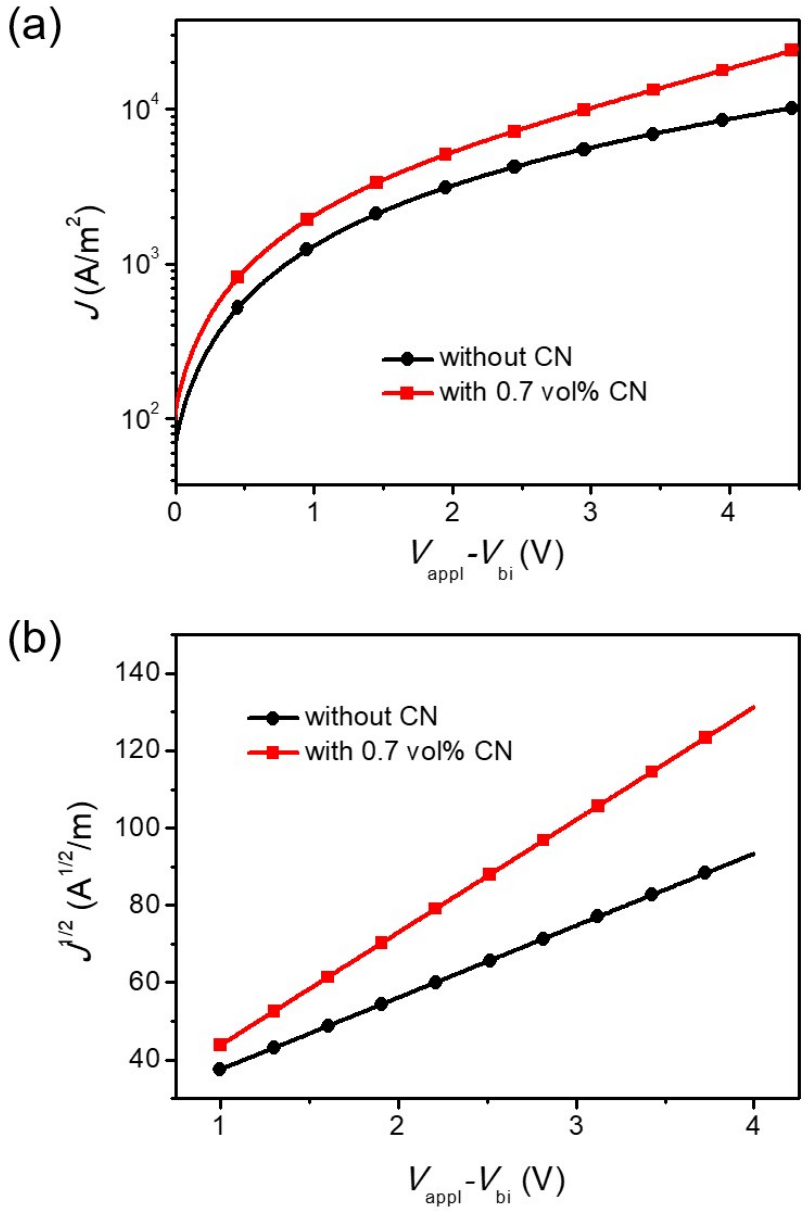

Fig. S9 *J*-*V* curves (a) and corresponding $J^{1/2}$-*V* plots (b) for the hole-only devices (in dark). The thicknesses for L1:IBCT (1:1.2) blend films without and with CN are 136 nm and 125 nm, respectively.

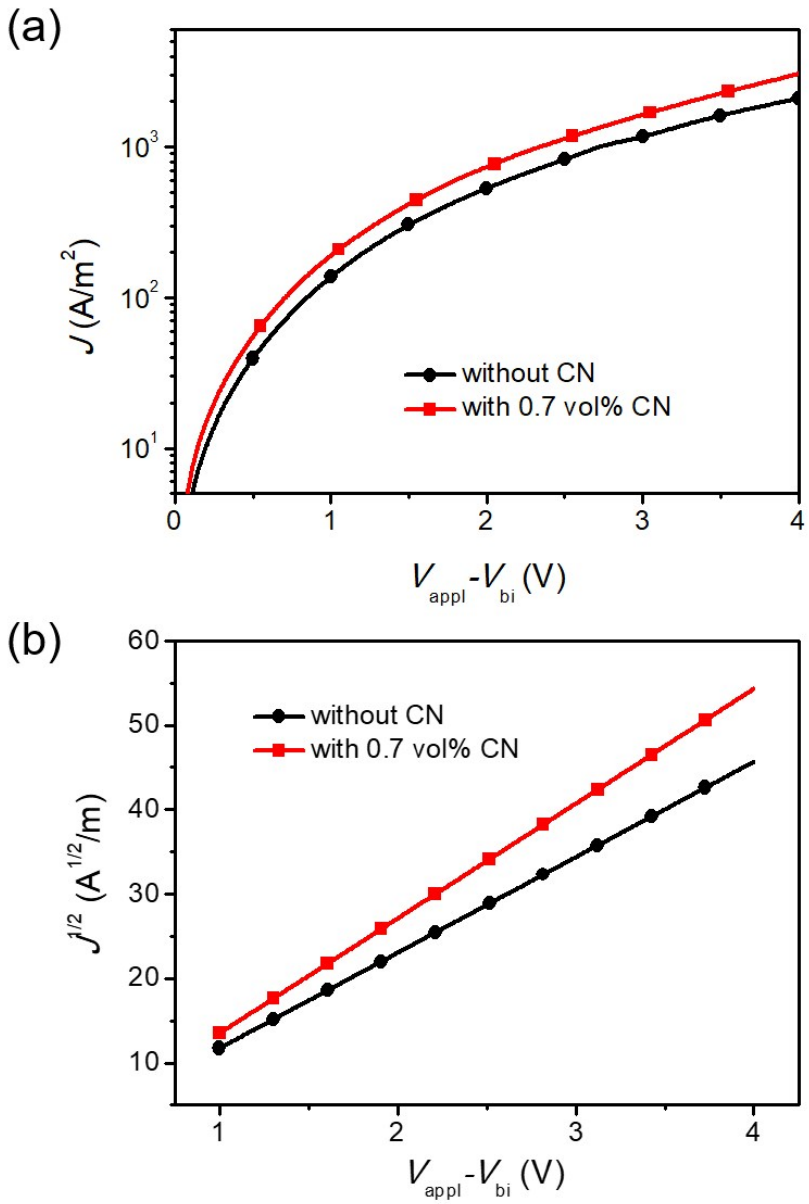

Fig. S10 *J-V* curves (a) and corresponding $J^{1/2}$-*V* plots (b) for the electron-only devices (in dark). The thicknesses for L1:IBCT (1:1.2) blend films without and with CN are 142 nm and 158 nm, respectively.

Table S4 Hole and electron mobilities.

Blend films	μ_h [cm^2/Vs]	μ_e [cm^2/Vs]	μ_h /μ_e
without CN	2.91×10^{-4}	1.23×10^{-4}	2.37
with 0.7% CN	5.56×10^{-4}	2.45×10^{-4}	2.27

9. Bimolecular recombination

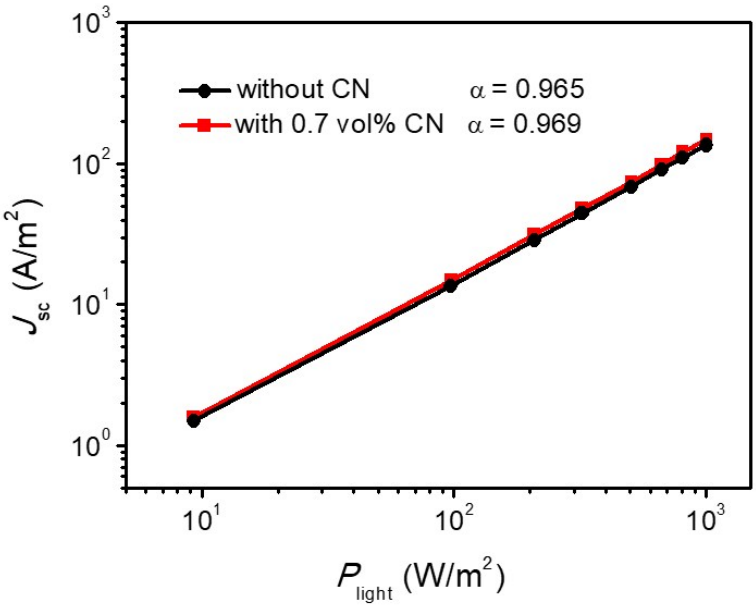

Fig. S11 J_{sc}-P_{light} plots.

10. AFM

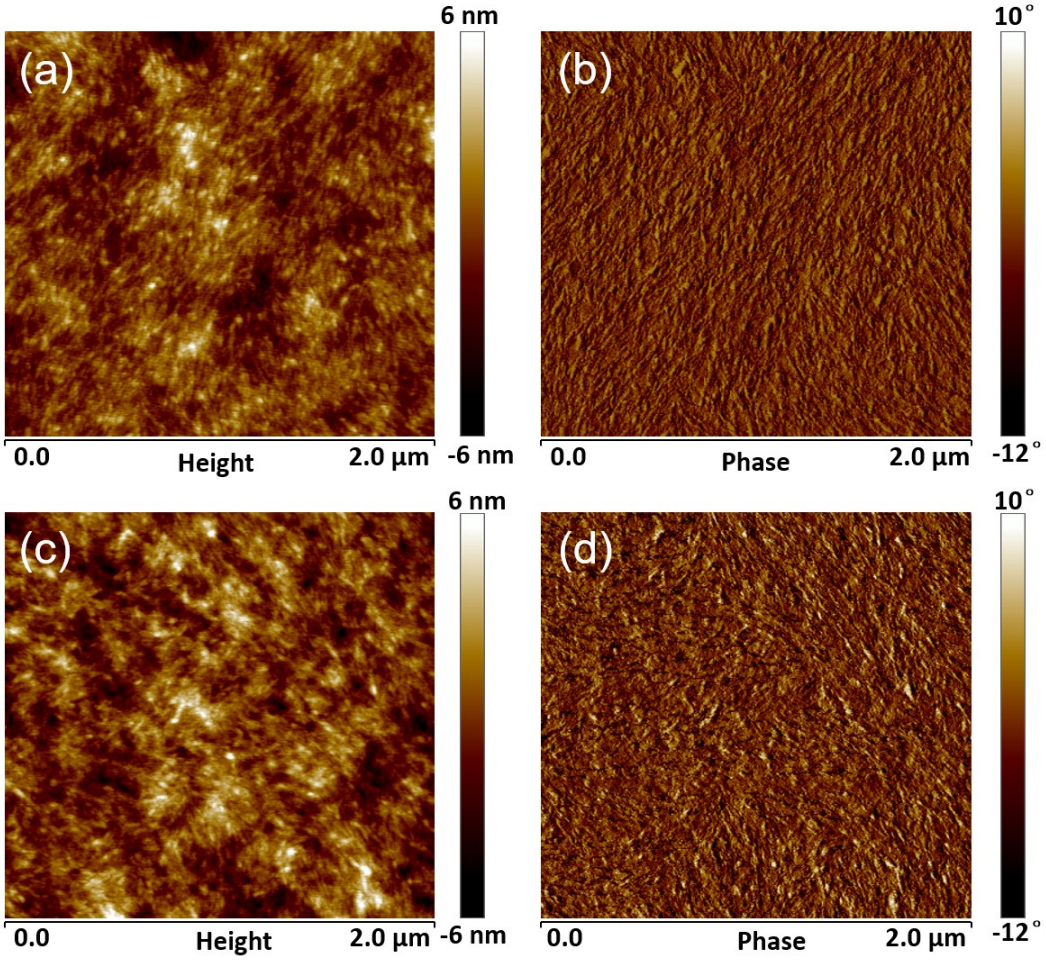

Fig. S12 AFM height (left) and phase (right) images for the blend films. (a) and (b), L1:IBCT film without CN (R_{rms} = 1.28 nm); (c) and (d), L1:IBCT film with 0.7 vol% CN (R_{rms} = 1.59 nm). R_{rms}: root-mean-square roughness.

11. A summary of the photovoltaic performance of reported medium-bandgap nonfullerene acceptors

Table S5 Solar cell performance of reported medium-bandgap (1.6 eV < E_g^{opt} < 1.9 eV) nonfullerene acceptors.

Acceptor	E_g^{opt} (eV)	Device structure	J_{sc} (mA/cm^2)	V_{oc} (V)	FF (%)	PCE (%)	Reference
IT-DM	1.61	ITO/ZnO/PBDB-T:IT-DM/MoO_3/Al	16.48	0.97	70.6	11.29	*Adv. Mater.,* 2016, **28**, 9423.
IDT6CN-Th	1.61	ITO/ZnO/PBDB-T:IDT6CNTh/MoO_3/Ag	16.75	0.81	76.72	10.41	*Adv. Mater.,* 2018, **30**, 1800052.
O-IDTBR	1.63	ITO/ZnO/P3HT:O-IDTBR/MoO_3/Ag	13.90	0.72	60.0	6.30	*Nat.Commun.,*2016, **7**, 11585.
FDICTF	1.63	ITO/PEDOT:PSS/PBDB-T:FDICTF/PDIN/Al	15.81	0.94	66.0	9.81	*Adv. Mater.,* 2017, **29**, 1604964 .
IT-OM-4	1.63	ITO/ZnO/PBDB-T:IT-OM-4/MoO_3/Al	14.69	0.96	56.0	7.90	*Adv. Energy Mater.,***7**, 2017, 1700183.
IDTBR	1.63	ITO/ZnO/PffBT4T-2DT:IDTBR/MoO_3/Ag	15.00	1.07	62.0	9.95	*Energy Environ. Sci.,* 2016, **9**, 3783.
IDT6CN	1.63	ITO/ZnO/PBDB-T:IDT6CN/MoO_3/Ag	15.14	0.83	73.77	9.27	*Adv. Mater.,* 2018, **30**, 1800052.
IDT-BOC6	1.63	ITO/ZnO/PBDB-T:IDT-BOC6/MoO_3/Al	17.52	1.01	54.0	9.60	*J. Am. Chem. Soc.,* 2017, **139**, 3356.
IT-OM-3	1.64	ITO/ZnO/PBDB-T:IT-OM-3/MoO_3/Al	16.38	0.97	68.0	10.80	*Adv. Energy Mater.,***7**, 2017, 1700183.
F-M	1.65	ITO/PEDOT:PSS/PBDB-T:F-M/PDINO/Al	14.56	0.98	71.0	10.08	*Adv. Mater.,* 2018, **30**, 1707508.
IDTI	1.65	ITO/PEDOT:PSS/PBDB-TF:IDTI/PFN-Br/Al	13.01	0.99	57.0	7.40	*Adv. Mater.,* 2017, **29**, 1704051.
IT-OM-1	1.67	ITO/ZnO/PBDB-T:IT-OM-1/MoO_3/Al	12.31	1.01	51.0	6.30	*Adv. Energy Mater.,***7**, 2017, 1700183.
ITCC	1.67	ITO/PEDOT:PSS/PBDB-T:ITCC/PFN-Br/Al	15.9	1.01	71.0	11.40	*Adv. Mater.,* 2017, **29**, 1700254.
H1	1.67	ITO/ZnO/P3HT:H1/LiF/Al	7.74	1.17	60.0	5.42	*Mater. Chem. Front.,* 2017, **1**, 1600.
IDTCN	1.67	ITO/ZnO/PBDB-T:IDTCN/MoO_3/Ag	12.06	0.85	62.48	6.40	*Adv. Mater.,* 2018, **30**, 1800052.
IDT-2BR	1.68	ITO/PEDOT:PSS/P3HT:IDT-2BR/Ca/Al	8.91	0.84	68.1	5.12	*Energy Environ. Sci.,* 2015, **8**, 3215.
ITCC-M	1.68	ITO/PEDOT:PSS/PBDB-T:ITCC-M/PFN-Br/Al	14.5	1.03	65.7	9.83	*J. Am. Chem. Soc.,* 2017, **139**, 7302.
IDT-HN	1.68	ITO/PEDOT:PSS/PBDB-T:IDT-HN/MoO3/Ag	14.43	0.93	76.41	10.22	*J. Mater. Chem. C,* 2018, **6**, 7046.
EH-IDTBR	1.68	ITO/ZnO/P3HT:EH-IDTBR/MoO_3/Ag	12.10	0.76	62.0	6.00	*Nat.Commun.,*2016, **7**, 11585.
IC-1IDT-IC	1.70	ITO/ZnO/PDBT-T1:IC-1IDT-IC/MoO_3/Al	13.39	0.92	60.0	7.39	*Adv. Energy Mater.,***6**, 2016, 1600854.
TfIF-IC-C8	1.70	ITO/PEDOT:PSS/PBDBT:TfIF-IC-C8/PFN-Br/Ag	13.21	0.97	66.67	8.57	*Organic Electronics,* 2019, **68**, 151.
		ITO/PEDOT:PSS/PBD					*Organic Electronics*

		BT:TfIF-IC-C2C6/PFN-Br/Ag					2019, **68**, 151.
TfIF-IC-C4C8	1.73	ITO/PEDOT:PSS/PBDBT:TfIF-IC-C4C8/PFN-Br/Ag	11.56	1.02	57.97	6.81	*Organic Electronics,* 2019, **68**, 151.
BTA3	1.76	ITO/PEDOT:PSS/J61:BTA3/Ca/Al	10.84	1.15	66.17	8.25	*Adv. Funct. Mater.,* 2018, **28**, 1704507.
BTA3	1.76	ITO/PEDOT:PSS/J52:BTA3/Ca/Al	14.62	1.07	60.34	9.41	*Chem. Mater.,* 2019, **31**, 3941.
BTA3	1.76	ITO/PEDOT:PSS/J52-Cl:BTA3/Ca/Al	13.16	1.24	66.62	10.50	*Chem. Mater.,* 2019, **31**, 3941.
SdiPBI-S	1.77	ITO/PEDOT:PSS/PDBT-T1:SdiPBI-S/Ca/Al	11.65	0.90	65.5	7.16	*J. Am. Chem. Soc.,* 2017, **137**, 11156.
DBFI-EDOT	1.77	ITO/ZnO/PEI/PSEHTT:DBFI-EDOT/MoO_3/Ag	13.82	0.93	63.0	8.10	*Adv. Mater.,* 2016, **28**, 124.
IDDT-TBA	1.78	ITO/ZnO/PBDB-T:IDDT-TBA/MoO_3/Ag	11.6 0	1.03	61 .0	7.30	*Sol. RRL.,* 2018, **2**, 1800120.
DICTF	1.82	ITO/PEDOT:PSS/PBDB-T:DICTF/PDIN/Al	10.30	0.93	59.0	5.65	*Adv. Mater.,* 2017, **29**, 1604964 .
BTA1	1.85	ITO/PEDOT:PSS/P3HT:BTA1/Ca/Al	7.34	1.02	70.0	5.24	*Adv. Energy Mater.,***7**, 2017, 1602269.
TPAPPDI	1.87	ITO/PEDOT:PSS/PBT1-EH:TPAPPDI/Ca/Al	6.84	1.22	61.8	5.10	*Sol. RRL.,* 2017, **1**, 1700123.
FTTB-PDI4	1.88	ITO/ZnO/P3TEA:FTTB-PDI4/V_2O_5/Al	13.89	1.13	65.9	10.58	*J. Am. Chem. Soc.,* 2017, **139**, 16092.

References

[1] Y. Lin, J. Wang, Z.-G. Zhang, H. Bai, Y. Li, D. Zhu and X. Zhan, *Adv. Mater.*, 2015, **27**, 1170-1174.

[2] W. J. E. Beek, M. M. Wienk, M. Kemerink, X. Yang and R. A. J. Janssen, *J. Phys. Chem. B*, 2005, **109**, 9505-9516.

[3] C. Duan, W. Cai, B. Hsu, C. Zhong, K. Zhang, C. Liu, Z. Hu, F. Huang, G. Bazan, A. J. Heeger and Y. Cao, *Energy Environ. Sci.*, 2013, **6**, 3022-3034.